Pharmaceutical Research, Vol. 8, No. 7, 1991

Research Article

Quantitative Evaluation of Ethanol Effects on Diffusion and Metabolism of β-Estradiol in Hairless Mouse Skin

Puchun Liu,[1] William I. Higuchi,[1,3] Wei-qi Song,[1] Tamie Kurihara-Bergstrom,[2] and William R. Good[1,2]

Received May 29, 1990; accepted February 9, 1991

The influence of low levels of ethanol on the simultaneous diffusion and metabolism of β-estradiol ($E_{2\beta}$) in hairless mouse skin was quantitatively evaluated. A wide range of diffusion/metabolism experiments was conducted with full-thickness skin, stripped skin, and dermis at the various ethanol levels. The experiments were carried out in a two-chamber diffusion-cell system where ethanol was present in both the donor and the receiver chambers at equal concentrations. Analysis of the experimental data with several enzyme distribution models further showed that the best model was that for which the enzyme activity resided totally in the epidermis and near the basal layer of the epidermis. The ethanol effects were separated and quantified in terms of the diffusion and metabolism parameters. Aqueous ethanol, even at low concentrations (≤25%), was found to have two important effects on $E_{2\beta}$ transport: ethanol functions as an inhibitor of the enzymatic conversion of $E_{2\beta}$ to estrone (E_1) in the viable epidermis, and ethanol is able to enhance the transport of permeants across the lipoidal pathway of the stratum corneum.

KEY WORDS: ethanol; diffusion enhancer; metabolism inhibitor; β-estradiol; hairless mouse skin; quantitative biophysical model.

INTRODUCTION

Recently, the diffusion and metabolism of β-estradiol ($E_{2\beta}$) in hairless mouse skin was quantified *in vitro* by the two-chamber diffusion cell experiments (1). In order to interpret the data, a general three-layer model with three possible enzyme distributions was considered (Fig. 1): Model A, Model B, and Model C. Analysis of all of the data showed that Model C was superior to Model B and Model A.

The influence of ethanol as a transport enhancer for $E_{2\beta}$ and other permeants in hairless mouse skin on a general basis was investigated recently (2,3). The experiments were carried out in a two-chamber diffusion cell system where ethanol was present in both the donor and the receiver chambers at equal concentrations. At high ethanol levels (>50%), a significant increase in new pore formation in the stratum corneum has been observed (3). At 100% ethanol, pore pathway diffusion dominated the permeation for all solutes, irrespective of polarity. At low ethanol levels (≤25%), there was no significant new pore formation; however, the diffusion of the solutes via the lipid pathway of the stratum corneum was greatly enhanced.

The objective of this research was to analyze the problem of how ethanol at low levels (≤25%) in both sides of the skin at equal concentrations may influence the simultaneous diffusion and metabolism of $E_{2\beta}$ (to estrone, E_1) in hairless mouse skin employing the recent baseline studies as a starting point. A question of particular interest was whether this study would also be consistent with Model C being superior to Model B and Model A.

MATERIALS AND METHODS

Much of the materials and methods information has been previously presented (1). Here, these are briefly described along with new information.

Materials

$E_{2\beta}$ and E_1 (Sigma Chemical Co., St Louis, MO) were used to make the standard mixtures in methanol (Baker Chemical Co., Phillipsburg, NJ). Normal saline (McGaw, Irvine, CA) and pure ethanol (US Industrial Chemical Co., Tuscola, IL) were used to prepare the solvent mixtures for all experiments (vol% of ethanol: 2, 8, 15, and 25). Analytical-grade acetonitrile (Baker Chemical Co., Phillipsburg, NJ) was used in the preparation of the HPLC mobile phase. Liquid scintillation fluid, Ready-Solv CP (Beckman Institute, San Ramon, CA), was used as obtained commercially. [6,7-^{3}H]$E_{2\beta}$ (60.0 Ci/mmol) and [6,7-^{3}H]E_1 (51.8 Ci/mmol) were obtained in their ethanol solutions from New England Nuclear, Boston, MA. The ethanol was evaporated with the

[1] Department of Pharmaceutics, University of Utah, Salt Lake City, Utah 84112.

[2] Pharmaceuticals Division, Ciba-Geigy Corporation, Ardsley, New York 10502.

[3] To whom correspondence should be addressed at Department of Pharmaceutics, Skaggs Hall 301, University of Utah, Salt Lake City, Utah 84112.

0724-8741/91/0700-0865$06.50/0

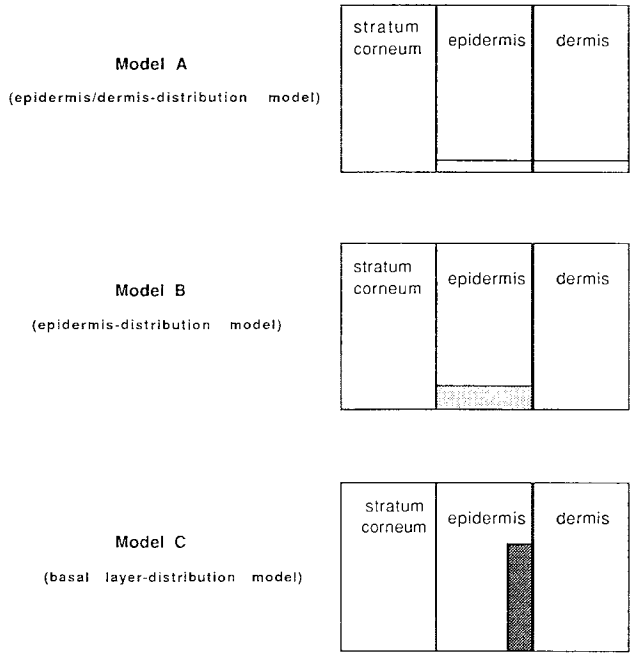

Fig. 1. Enzyme distribution models used in data interpretation.

aid of a nitrogen stream before ^{3}H-$E_{2\beta}$ or ^{3}H-E_1 was used for diffusion/metabolism experiments.

Male hairless mice (strain SKH-HR1) at ages of 12–15 weeks old were obtained from Temple University, Philadelphia, PA.

Skin Membrane Preparations

The mouse was sacrificed by spinal dislocation. Two pieces of skin preparation were obtained from the abdominal region of each mouse. Three kinds of fresh membranes (full-thickness skin, stripped skin, and dermis) were prepared. Full-thickness skin, consisting of stratum corneum, viable epidermis, and dermis, was obtained freed from adhering fat and other debris. Stripped skin, consisting of the epidermis and the dermis, was obtained after the stratum corneum was removed by a cellophane tape (Scotch tape, 3M Co., St. Paul, MN) stripping technique (4). Dermis was obtained by removing the epidermal half of the skin using a dermatome (4). The dermis thickness was measured with a micrometer after the experiment by sandwiching the membrane between two glass slides (4).

Diffusion/Metabolism Experiments

The diffusion/metabolism experiments were conducted using a two-chamber diffusion cell (5) with the ethanol/saline compositions the same in the donor and the receiver chambers. The experiments were carried out with two permeants ($E_{2\beta}$ and E_1), three skin membranes (dermis, stripped skin, and full-thickness skin), and two membrane configurations (configuration 1, dermis facing the receiver chamber; and configuration 2, dermis facing the donor chamber). In each chamber, a stainless-steel (Carpenter stainless type 316L) stirrer with a small stainless-steel propeller was affixed to a 150-rpm constant-speed motor. The skin membranes were sandwiched between the half cells and clamped. In a typical experiment, exactly 2.0 ml of an ethanol/saline solution was pipetted into both the donor and the receiver chambers and allowed to equilibrate for 10 min at 37°C. A predetermined amount of ^{3}H-$E_{2\beta}$ or ^{3}H-E_1 was then added into the donor chamber and aliquots were withdrawn from the receiver chamber at predetermined time intervals after steady state was attained. The same volume of ethanol/saline solution was added back to the receiver chamber to keep a constant volume. Except when taking a sample, the sample port was covered to avoid evaporation during the experimental period. The receiver chamber was always kept at sink conditions ($\lesssim$10% of the donor concentration).

HPLC-Fraction Collector-Liquid Scintillation Counting

Separation of ^{3}H-$E_{2\beta}$ or ^{3}H-E_1 was performed by interfacing the HPLC (high-performance liquid chromatograph) with a fraction collector. The HPLC system was a V4 variable wavelength absorbance detector (ISCO, Lincoln, NE), a 110B solvent delivery module (Beckman Institute, San Ramon, CA), and a C6W injector (Valco Institute, San Antonio, TX). The species were resolved by a reversed-phase column, Resolvex C18 (10 μm), 250 × 4.6 mm (Fisher Scientific Co., Pittsburg, PA) with acetonitrile–water (40:60) at wavelength 280 nm. The radioactive samples were mixed with the nonradioactive standard mixture solution to give the HPLC chromatograms. Each species was collected on a FOXY fraction collector (ISCO, Lincoln, NE) with mode 3 and cycle 0. The fraction collector was programmed to give fraction sizes based on the peak signals from the ISCO detector with a built-in peak separator. Each fraction was analyzed by liquid scintillation counting (Beckman LS 750, Beckman Institute, San Ramon, CA).

RESULTS AND DISCUSSION

Influence of Ethanol on Experimental Fluxes

At steady state, the following equations were used to calculate the forward fluxes for the drug ($J_{A,f}$) and the metabolite ($J_{B,f}$) and the back flux for the metabolite ($J_{B,b}$) from the experimental transport/metabolism data:

$$J_{A,f} = \frac{(dA_{A,R}/dt)}{S} \quad (1)$$

$$J_{B,f} = \frac{(dA_{B,R}/dt)}{S} \quad (2)$$

$$J_{B,b} = \frac{(dA_{B,D}/dt)}{S} \quad (3)$$

Here S is the effective diffusion area, $A_{A,R}$ is the drug amount transported into the receiver chamber, $A_{B,R}$ and $A_{B,D}$ are the metabolite amounts transported into the receiver and the donor chambers, respectively, and t represents time.

Equations (1) to (3) may underestimate the correct fluxes because the amount of permeant retained in the epidermis/dermis is not negligible compared to the permeant in the receiver chamber. A procedure for correcting the flux values was recently developed (1,6), and it has been applied where appropriate to the experimental data.

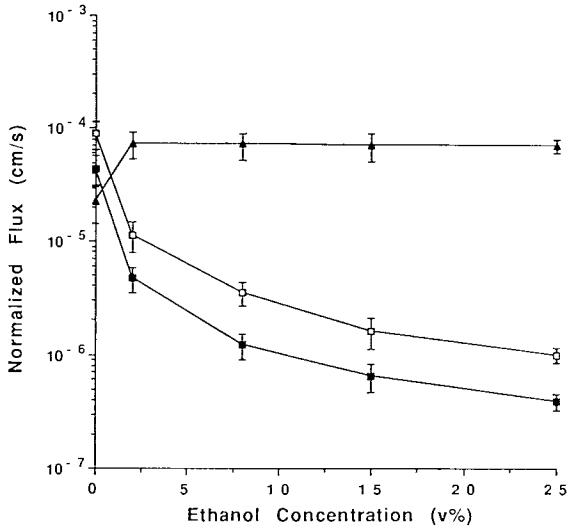

Fig. 2. Influence of ethanol on the normalized forward flux of $E_{2\beta}$ (▲) and on the normalized forward flux (■) and back flux (□) of its transdermal metabolite, E_1, with stripped hairless mouse skin in configuration 1. Each data point represents the mean and standard deviation of four determinations.

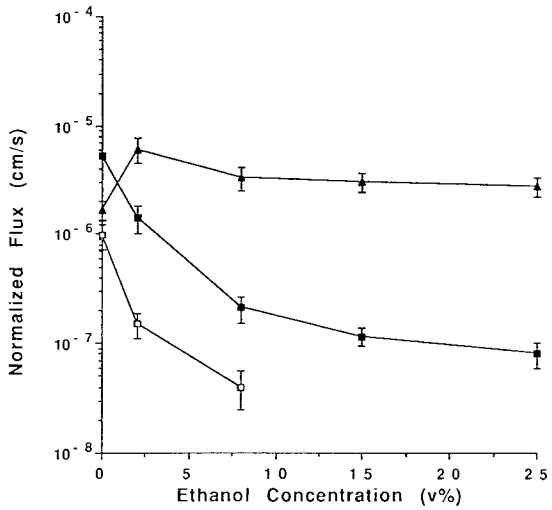

Fig. 4. Influence of ethanol on the normalized forward flux of $E_{2\beta}$ (▲) and on the normalized forward flux (■) and back flux (□) of its transdermal metabolite, E_1, with full-thickness hairless mouse skin in configuration 1. Each data point represents the mean and standard deviation of four determinations.

Normalized fluxes are defined as the fluxes given by Eqs. (1) to (3) divided by the donor concentration of the permeant/substrate. In the case of experiments of either $E_{2\beta}$ or E_1 with the dermis membrane, no significant metabolism was found and the normalized forward fluxes of $E_{2\beta}$ and E_1 are, therefore, simply equal to the dermis permeability coefficients of $E_{2\beta}$ and E_1, respectively, which (as shown later) are essentially the same.

Figures 2–5 summarize the observed normalized fluxes determined in diffusion/metabolism experiments with stripped skin and with full-thickness skin in the cases where $E_{2\beta}$ is the permeant/substrate. Some of the main features of these data are the following. First, the influence of ethanol on transdermal metabolism is strong in all cases. Even at 2%, ethanol inhibits the $E_{2\beta} \rightarrow E_1$ metabolism by a factor of 10 in terms of both forward and back fluxes of E_1. Second, with stripped skin the ratio of the back-to-forward fluxes of the metabolite (E_1) is significantly greater for configuration 1 (Fig. 2) than for configuration 2 (Fig. 3). This result may be explained by little or no metabolic activity in the dermis (1), which serves only as a diffusion barrier; therefore, enzyme

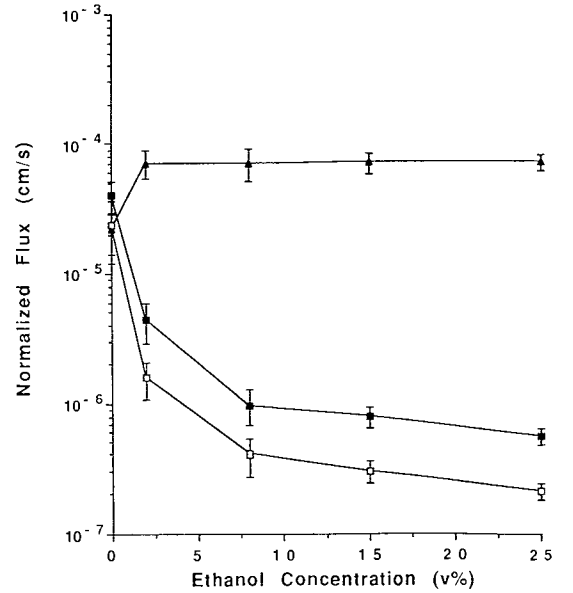

Fig. 3. Influence of ethanol on the normalized forward flux of $E_{2\beta}$ (▲) and on the normalized forward flux (■) and back flux (□) of its transdermal metabolite, E_1, with stripped hairless mouse skin in configuration 2. Each data point represents the mean and standard deviation of four determinations.

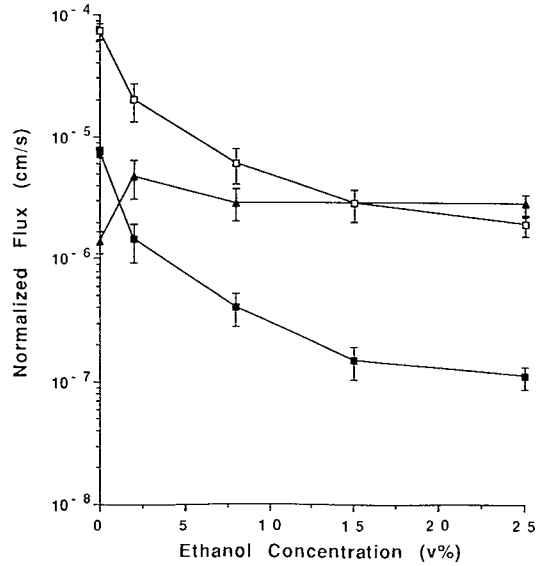

Fig. 5. Influence of ethanol on the normalized forward flux of $E_{2\beta}$ (▲) and on the normalized forward flux (■) and back flux (□) of its transdermal metabolite, E_1, with full-thickness hairless mouse skin in configuration 2. Each data point represents the mean and standard deviation of four determinations.

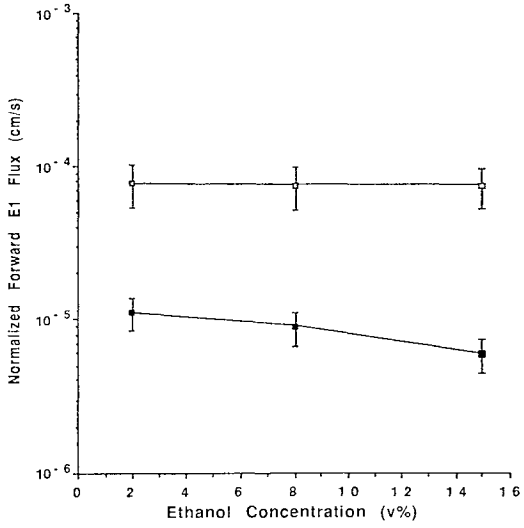

Fig. 6. Influence of ethanol on the normalized forward fluxes of E_1 with hairless mouse stripped skin (□) and full-thickness skin (■) in configuration 1. The forward and back fluxes of $E_{2\beta}$ (not shown here), the metabolite of E_1, generated during E_1 transport through the skin, were <5% (in 15% ethanol case) to 10% (in 2% ethanol case) of the E_1 fluxes.

access by substrate, metabolism, and back diffusion of metabolite is greater for configuration 1 than for configuration 2. Finally, with the full-thickness skin data, the strong influence of the stratum corneum as a transport barrier can be seen. As the permeability coefficient of the stratum corneum is significantly smaller than that of dermis, the ratio of the back-to-forward fluxes of metabolite (E_1) is much greater for configuration 2 (Fig. 5) than for configuration 1 (Fig. 4), this being the opposite of the stripped skin results discussed above.

Figure 6 summarizes the experiments in which E_1 was the permeant/substrate. Only the forward-flux data for E_1 are presented because conversion $E_1 \rightarrow E_{2\beta}$ was lower and because, even at 2% ethanol, the fluxes of $E_{2\beta}$ were less than 5 to 10% of those of E_1.

Analysis of Model with the Experimental Data

The model approach was previously presented (1) and used in the analysis of experiments on the simultaneous transport and metabolism of $E_{2\beta}$ in hairless mouse skin. The present situation differs in that it involves the examination of the influence of ethanol on both the transport parameters and the metabolism parameters in the models.

The model for hairless mouse skin is composed of n layers where n may be three or four. In the steady state, we may write

$$D_{2\beta,i}\frac{d^2C_{2\beta}}{dx^2} - k_iC_{2\beta} = 0 \quad (4)$$

$$D_{1,i}\frac{d^2C_1}{dx^2} + k_iC_{2\beta} = 0 \quad (5)$$

where the D's are the diffusion coefficients and the k's are the first-order enzyme rate constants. The C's are the concentrations and the coordinate $x[0 \leq x \leq h(\text{thickness})]$ is the depth in the membrane. The subscripts 2β and 1 refer to the $E_{2\beta}$ and E_1 and i refers to the ith layer of the skin. Full-thickness skin is then considered as a three-layer (stratum corneum, epidermis, and dermis) or a four-layer (stratum corneum, basal layer of epidermis, the remainder of the epidermis, and dermis) membrane as depicted by Model A, Model B, or Model C (see Fig. 1). The D's and k's, in general, may have different values for the different components of a membrane, but they are assumed to be constant within

Table I. Analysis of Model B and Model C with Experimental Fluxes in Saline Case: Diffusion and Metabolism Parameters Deduced from the Models[a]

Model	Parameter	Stripped skin, Configuration[b] 1	Stripped skin, Configuration[b] 2	Full-thickness skin, Configuration[b] 1	Full-thickness skin, Configuration[b] 2	Average
B	$k \times 10$	1.10 ± 0.20	6.60 ± 1.60	1.01 ± 0.32	2.99 ± 0.41	3.05 ± 3.05*
	$P_{2\beta,e} \times 10^4$	7.61 ± 1.41	23.1 ± 9.60			15.4 ± 11.4*
	$P_{1,e} \times 10^4$	0.21 ± 0.07[c]	6.45 ± 1.82			3.33 ± 3.62*
	$P_{2\beta,s} \times 10^6$			9.70 ± 3.15	2.12 ± 0.64	5.91 ± 4.64*
	$P_{1,s} \times 10^6$			0.94 ± 0.29[c]	9.52 ± 2.02	5.23 ± 4.88*
C	$k \times 10$	8.20 ± 1.40	6.90 ± 1.50	7.00 ± 1.30	6.30 ± 1.80	7.10 ± 2.02
	$P_{2\beta,e} \times 10^4$	2.18 ± 0.43	1.99 ± 0.75			2.09 ± 0.73
	$P_{1,e} \times 10^4$	2.47 ± 0.86	2.16 ± 0.71			2.32 ± 0.73
	$P_{2\beta,s} \times 10^6$			9.42 ± 1.20	8.36 ± 1.91	8.89 ± 1.93
	$P_{1,s} \times 10^6$			10.8 ± 1.39	11.5 ± 2.53	11.1 ± 2.75

[a] Model B, the enzyme is homogeneously distributed in the epidermis; Model C, the enzyme is located in the basal layer of the epidermis near the dermoepidermal junction. Parameters [k, first-order enzyme rate constant (sec^{-1}), $P_{2\beta,e}$ and $P_{1,e}$, epidermis permeability coefficient (cm/sec) of $E_{2\beta}$ and E_1; and $P_{2\beta,s}$ and $P_{1,s}$, stratum corneum permeability coefficient (cm/sec) of $E_{2\beta}$ and E_1] are expressed as the mean ± SD (n = 4) and determined with the dermis permeability coefficient of $E_{2\beta}$ and E_1: $P_{2\beta,d} = 1.0 \times 10^{-4}$ cm/sec and $P_{1,d} = 1.1 \times 10^{-4}$ cm/sec.

[b] Configuration 1: stratum corneum → epidermis → dermis. Configuration 2: dermis → epidermis → stratum corneum.

[c] Out of the physical meaningful range.

* Significantly different.

Table II. Analysis of Model B and Model C with Experimental Fluxes in 2% Ethanol Case: Diffusion and Metabolism Parameters Deduced from the Models[a]

Model	Parameter	Stripped skin, Configuration[b] 1	Stripped skin, Configuration[b] 2	Full-thickness skin, Configuration[b] 1	Full-thickness skin, Configuration[b] 2	Average
B	$k \times 10^2$	0.96 ± 0.20	1.45 ± 0.30	1.05 ± 0.22	1.15 ± 0.24	1.15 ± 0.33
	$P_{2\beta,e} \times 10^4$	1.95 ± 0.67	1.66 ± 0.61			1.81 ± 0.60
	$P_{1,e} \times 10^4$	0.76 ± 0.25	2.11 ± 0.71			1.43 ± 0.89*
	$P_{2\beta,s} \times 10^6$			7.43 ± 2.35	7.42 ± 2.27	7.42 ± 2.06
	$P_{1,s} \times 10^6$			6.29 ± 1.57	8.30 ± 2.19	7.30 ± 2.04
C	$k \times 10^2$	4.10 ± 1.03	3.56 ± 0.72	3.50 ± 0.53	4.00 ± 0.68	3.79 ± 0.60
	$P_{2\beta,e} \times 10^4$	2.00 ± 0.69	2.43 ± 0.61			2.22 ± 0.63
	$P_{1,e} \times 10^4$	1.89 ± 0.73	2.23 ± 0.63			2.06 ± 0.64
	$P_{2\beta,s} \times 10^6$			8.03 ± 0.91	6.56 ± 1.33	7.29 ± 1.31
	$P_{1,s} \times 10^6$			10.3 ± 1.08	10.3 ± 1.75	10.3 ± 1.31

[a] See Table I, footnote *a*.
[b] See Table I, footnote *b*.
* Significantly different.

a particular membrane component or a subcomponent. The thicknesses are assigned values of 20, 20, and 250 μm for stratum corneum, epidermis, and dermis, respectively. For Model C, the basal layer will be assumed to be the lower one-third of the epidermis.

Equations (4) and (5) may be solved analytically or numerically as described previously (1) when the experimental flux data are available. With boundary concentrations, computer iterations were done to fit the calculated fluxes to the experimental data. Three parameters were adjusted in best-fitting the data from each set of experiments to each model. The epidermis permeability coefficients for $E_{2\beta}$ and E_1 and the first-order enzyme rate constant were first simultaneously deduced using stripped skin experimental fluxes and the predetermined dermis permeability coefficients of $E_{2\beta}$ and E_1. Then these predetermined epidermis and dermis permeability coefficients were used with the full-thickness skin experimental fluxes to deduce simultaneously the "best" values for the stratum corneum permeability coefficients of $E_{2\beta}$ and E_1 and the enzyme rate constant.

In the discussion that follows, the results of model analysis for Model B and Model C are presented; Model A may be eliminated because of negligible enzyme activity in the dermis. The comparisons of the experimental data with Model B and Model C are presented in Tables I–V for ethanol levels from 0 to 25%.

Previously (1), it was argued that Model C was clearly better than Model B when the solvent was pure saline. This situation is reviewed in Table I, which shows that the various parameter values deduced from the several independent experiments were consistently much more constant when they were deduced using Model C than with Model B. Essentially all parameter values in Table I for Model B varied far beyond the experimental uncertainties, while all parameter values for Model C were constant within their respective standard deviations.

Table III. Analysis of Model B and Model C with Experimental Fluxes in 8% Ethanol Case: Diffusion and Metabolism Parameters Deduced from the Models[a]

Model	Parameter	Stripped skin, Configuration[b] 1	Stripped skin, Configuration[b] 2	Full-thickness skin, Configuration[b] 1	Full-thickness skin, Configuration[b] 2	Average
B	$k \times 10^3$	2.50 ± 0.63	3.20 ± 0.81	2.98 ± 0.65	3.00 ± 0.74	2.92 ± 0.66
	$P_{2\beta,e} \times 10^4$	2.02 ± 0.70	2.17 ± 0.75			2.10 ± 0.65
	$P_{1,e} \times 10^4$	0.62 ± 0.21	1.04 ± 0.36			0.84 ± 0.35
	$P_{2\beta,s} \times 10^6$			3.48 ± 0.86	3.24 ± 0.74	3.36 ± 0.73
	$P_{1,s} \times 10^6$			7.59 ± 1.84	5.76 ± 1.23	6.67 ± 1.73
C	$k \times 10^3$	9.48 ± 2.96	12.4 ± 3.69	8.01 ± 2.99	8.56 ± 1.87	9.61 ± 3.07
	$P_{2\beta,e} \times 10^4$	2.36 ± 0.52	1.77 ± 0.42			2.13 ± 0.58
	$P_{1,e} \times 10^4$	2.86 ± 0.74	1.84 ± 0.45			2.30 ± 0.77
	$P_{2\beta,s} \times 10^6$			3.30 ± 0.76	3.50 ± 1.07	3.41 ± 0.84
	$P_{1,s} \times 10^6$			9.24 ± 1.84	7.33 ± 2.09	8.28 ± 2.04

[a] See Table I, footnote *a*.
[b] See Table I, footnote *b*.

Table IV. Analysis of Model B and Model C with Experimental Fluxes in 15% Ethanol Case: Diffusion and Metabolism Parameters Deduced from the Models[a]

Model	Parameter	Stripped skin, Configuration[b] 1	Stripped skin, Configuration[b] 2	Full-thickness skin, Configuration[b] 1	Full-thickness skin, Configuration[b] 2	Average
B	$k \times 10^3$	1.74 ± 0.35	3.02 ± 0.61	1.54 ± 0.31	1.35 ± 0.27	1.91 ± 0.77
	$P_{2\beta,e} \times 10^4$	2.05 ± 0.64	2.11 ± 0.67			2.08 ± 0.57
	$P_{1,e} \times 10^4$	1.22 ± 0.44	1.33 ± 0.41			1.28 ± 0.39
	$P_{2\beta,s} \times 10^6$			3.25 ± 0.80	3.19 ± 0.73	3.22 ± 0.69
	$P_{1,s} \times 10^6$			5.98 ± 1.39	4.71 ± 1.18	5.35 ± 1.35
C	$k \times 10^3$	5.00 ± 0.58	4.09 ± 0.83	6.63 ± 0.62	5.30 ± 1.00	5.11 ± 1.12
	$P_{2\beta,e} \times 10^4$	2.05 ± 0.82	1.95 ± 0.32			2.10 ± 0.53
	$P_{1,e} \times 10^4$	1.85 ± 0.21	2.36 ± 0.62			2.09 ± 0.49
	$P_{2\beta,s} \times 10^6$			3.23 ± 0.64	3.20 ± 0.85	3.22 ± 0.67
	$P_{1,s} \times 10^6$			6.40 ± 1.07	5.36 ± 1.58	5.88 ± 1.33

[a] See Table I, footnote *a*.
[b] See Table I, footnote *b*.

In the presence of ethanol, it is apparent from examining Tables II–V that Model C is generally better than Model B, especially at the lower ethanol levels. However, the superiority of Model C over Model B is much less clear when ethanol is present than when the experiments are run in saline alone. It is believed that this poorer distinguishability between Model C and Model B in the presence of ethanol is related mainly to the fact that, when the metabolism rates are high, the distinguishability between Model C and Model B is great but when the metabolism rates are reduced, the distinguishability is poor. This concept is illustrated in Table VI; it was assumed that Model C was valid and Model B was used to deduced the Model B parameters. As can be seen from the last column in Table VI, Ratio (conf. 2/conf. 1), when metabolism rates are large, the Model B deduced parameter values (k, $P_{e,2\beta}$, and $P_{e,1}$) for configuration 1 and for configuration 2 differ much more than when the metabolism rates are low.

Ethanol Effects on the Parameters for Diffusion and Metabolism

The transport parameters obtained using Model C are presented in Fig. 7. Here the epidermis and stratum corneum permeability coefficients for $E_{2\beta}$ and E_1 are presented along with the dermis permeability coefficients that were obtained from dermis transport experiments and corrected to 250-μm thickness.

It is seen that both the epidermis and the dermis permeability coefficients are relatively independent of the ethanol concentration. In view of the strong dependencies of the thermodynamic activity coefficient for $E_{2\beta}$ or E_1 upon ethanol concentration, these results are best explained by considering both epidermis and dermis to limit transport via aqueous/ethanol pore pathways (3).

The modest decreases in the stratum corneum permeability coefficients for $E_{2\beta}$ and E_1 may be explained by a

Table V. Analysis of Model B and Model C with Experimental Fluxes in 25% Ethanol Case: Diffusion and Metabolism Parameters Deduced from the Models[a]

Model	Parameter	Stripped skin, Configuration[b] 1	Stripped skin, Configuration[b] 2	Full-thickness skin, Configuration[b] 1	Full-thickness skin, Configuration[b] 2	Average
B	$k \times 10^3$	1.00 ± 0.21	1.81 ± 0.37	0.99 ± 0.20	1.01 ± 0.24	1.20 ± 0.43
	$P_{2\beta,e} \times 10^4$	1.90 ± 0.48	1.98 ± 0.60			1.94 ± 0.39
	$P_{1,e} \times 10^4$	1.08 ± 0.31	1.52 ± 0.30			1.30 ± 0.36
	$P_{2\beta,s} \times 10^6$			3.00 ± 0.75	3.00 ± 0.60	3.00 ± 0.68
	$P_{1,s} \times 10^6$			5.50 ± 1.38	3.50 ± 1.98	4.76 ± 1.11
C	$k \times 10^3$	3.30 ± 0.60	3.50 ± 0.40	3.43 ± 0.51	3.42 ± 0.68	3.41 ± 0.48
	$P_{2\beta,e} \times 10^4$	2.10 ± 0.40	1.92 ± 0.35			2.01 ± 0.35
	$P_{1,e} \times 10^4$	2.05 ± 0.45	1.93 ± 0.30			1.99 ± 0.35
	$P_{2\beta,s} \times 10^6$			3.11 ± 0.60	2.89 ± 0.59	3.00 ± 0.55
	$P_{1,s} \times 10^6$			5.56 ± 1.10	5.40 ± 0.98	5.48 ± 0.94

[a] See Table I, footnote *a*.
[b] See Table I, footnote *b*.

Table VI. Calculations Showing That the Distinguishability Between Model C and Model B Is Greater at High Metabolism Rates[a]

Case[b]	Parameter[a]	Conf. 1	Conf. 2	Ratio (Conf. 2/Conf. 1)
8	k (sec^{-1})	0.53	4.05	7.6
	$P_{2\beta,e}$ (cm/sec)	5.90×10^{-5}	3.10×10^{-4}	5.3
	$P_{1,e}$ (cm/sec)	3.00×10^{-6}	1.65×10^{-4}	55
0.8	k (sec^{-1})	0.13	0.45	3.5
	$P_{2\beta,e}$ (cm/sec)	1.10×10^{-4}	2.60×10^{-4}	2.4
	$P_{1,e}$ (cm/sec)	4.00×10^{-5}	1.40×10^{-4}	3.5
0.08	k (sec^{-1})	0.02	0.045	2.3
	$P_{2\beta,e}$ (cm/sec)	1.70×10^{-4}	2.10×10^{-4}	1.2
	$P_{1,e}$ (cm/sec)	6.50×10^{-5}	1.20×10^{-4}	1.9
0.008	k (sec^{-1})	0.002	0.004	2.0
	$P_{2\beta,e}$ (cm/sec)	1.97×10^{-4}	2.00×10^{-4}	1.0
	$P_{1,e}$ (cm/sec)	7.00×10^{-5}	1.20×10^{-4}	1.7
0.0008	k (sec^{-1})	0.0002	0.0004	2.0
	$P_{2\beta,e}$ (cm/sec)	2.00×10^{-4}	2.00×10^{-4}	1.0
	$P_{1,e}$ (cm/sec)	7.00×10^{-5}	1.20×10^{-4}	1.7

[a] Model C was assumed to be absolutely correct and Model B was used to deduce Model B parameters (k, first-order enzyme rate constant; $P_{2\beta,e}$ and $P_{1,e}$, epidermis permeability coefficient of $E_{2\beta}$ and E_1) with stripped skin.

[b] These numbers are the Model C k values; also, Model C $P_{2\beta,e} = P_{1,e} = 2 \times 10^{-4}$ cm/sec.

combination of two opposing factors: (a) transport via a lipoidal pathway which results in rather large decreases in the thermodynamic activities of the two permeants when partitioning favors the solvent phase in the presence of ethanol and (b) significant transport enhancement by ethanol. Ghanem *et al.* (3) have shown that $E_{2\beta}$, E_1, and other permeants may be enhanced about 8- to 10-fold by ethanol at 25%; the present data are consistent with their findings. The ethanol enhancement of $E_{2\beta}$, E_1, and ethanol itself has been observed both in hairless mouse stratum corneum and in human stratum corneum (6).

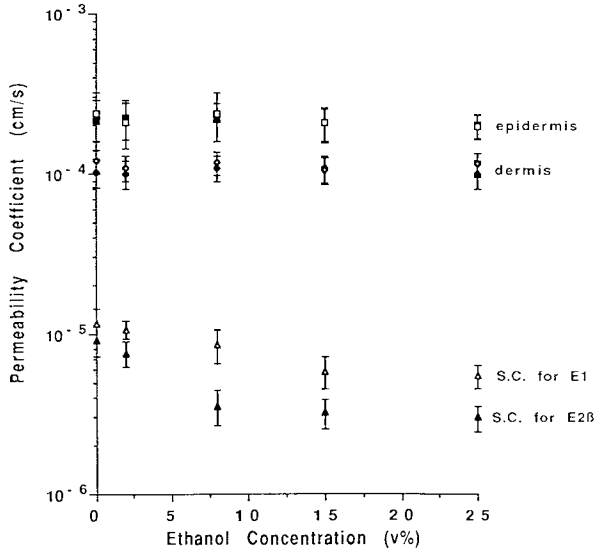

Fig. 7. Ethanol effect on the intrinsic permeability coefficients of $E_{2\beta}$ (filled symbols) and of E_1 (open symbols) with dermis (◇, ◆), epidermis (□, ■), and stratum corneum (△, ▲). Each data point of dermis (normalized thickness, 250 μm), determined directly with $E_{2\beta}$ and E_1, represents the mean and standard deviation of three or four determinations (either configuration 1 or configuration 2). Each data point of epidermis and stratum corneum represents the mean and standard deviation of eight determinations.

The apparent first-order enzyme rate constants (k) deduced from Model C are shown in Fig. 8 for all ethanol levels. Numerically, the decrease in k as a function of ethanol concentration (C_{EtOH}) may be described by a competitive inhibition kinetics expression:

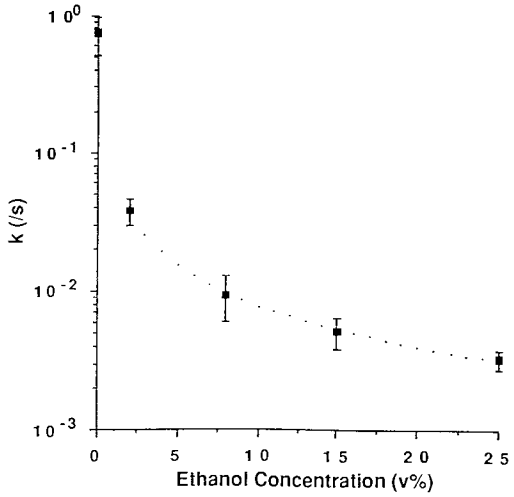

Fig. 8. Ethanol effect on the intrinsic first-order enzyme rate constant in the basal layer of epidermis with $E_{2\beta}$. Each data point represents the mean and standard deviation of 16 determinations. The dotted curve is Eq. (6) with a k_{in} value of 0.10%.

$$k = \frac{k_0}{1 + (C_{EtOH}/k_{in})} \quad (6)$$

where the intrinsic enzyme rate constant, k_0, was determined from the saline experiment to be about 0.70 sec^{-1} and the inhibition rate constant, k_{in}, was calculated to be about 0.10 (vol%) by curve-fitting.

As it is known that the solubility of estradiol increases greatly with increasing ethanol concentration (2), it was thought that the enzyme inhibition may be partly related to this phenomenon (i.e., the lowering of the chemical potential of $E_{2\beta}$ with increasing ethanol). When ethanol concentration increases from 0 to 25%, there is an approximately 20-fold increase in $E_{2\beta}$ solubility (2,3). This, however, is not sufficient to account for the more than 200 times decrease in the enzyme rate constant, k (Fig. 8). It is noteworthy that 17β-hydroxysteroid dehydrogenase is an enzyme in rat skin (7) catalyzing the $E_{2\beta} \rightarrow E_1$ reaction. The enzyme, located in skin microsomes, has a preference of NADP as cofactor. Acute ethanol exposure has been reported to inhibit the action of mixed function oxidase in rat hepatic microsomes (8,9). This inhibition has been interpreted as competitive kinetics by some investigators (10,11).

CONCLUSION

Ethanol participates in two important ways with regard to the transport and metabolism of $E_{2\beta}$ in skin. It acts as a transport enhancer for $E_{2\beta}$ across the stratum corneum and acts as an inhibitor of the metabolic conversion of $E_{2\beta} \rightarrow E_1$ in the epidermis. In the present study, the usefulness of the physical model approach is demonstrated in gaining insights and in quantifying the transport and metabolism of $E_{2\beta}$ in hairless mouse skin. The analysis strongly supports the specific model (Model C) in which the metabolic conversion of $E_{2\beta} \rightarrow E_1$ and the ethanol inhibition of this biochemical reaction take place in the basal layer of the epidermis.

ACKNOWLEDGMENTS

This research was supported by the Ciba-Geigy Corp. (Ardsley, New York). P. Liu was supported in part by the University of Utah Graduate Research Fellowship (1987–1988).

REFERENCES

1. P. Liu, W. I. Higuchi, A. H. Ghanem, T. Kurihara-Bergstrom, and W. R. Good. Quantitation of simultaneous diffusion and metabolism of β-estradiol in hairless mouse skin: Enzyme distribution and intrinsic diffusion/metabolism parameters. *Int. J. Pharm.* 64:7–25 (1990).
2. W. I. Higuchi, U. D. Rohr, S. A. Burton, P. Liu, J. L. Fox, A. H. Ghanem, H. Mahmoud, S. Borsadia, and W. R. Good. The effects of ethanol on transport of β-estradiol in hairless mouse skin. I. Comparison of experimental data with a pore model. In P. I. Lee and W. R. Good (eds.), *Controlled Release Technology, Pharmaceutical Applications,* ACS Symp. Ser. 348, American Chemical Society, Washington, D.C., 1987, pp. 232–240.
3. A. H. Ghanem, H. Mahmoud, W. I. Higuchi, U. D. Rohr, S. Borsadia, P. Liu, J. L. Fox, and W. R. Good. The effects of ethanol on transport of β-estradiol and other permeants in hairless mouse skin. *J. Control. Rel.* 6:75–83 (1987).
4. C. D. Yu, J. L. Fox, N. F. H. Ho, and W. I. Higuchi. Physical model evaluation of topical prodrug delivery—simultaneous transport and bioconversion of vidarabine 5′-valerate. II. Parameter determinations. *J. Pharm. Sci.* 68:1347–1357 (1979).
5. H. Durrheim, G. L. Flynn, W. I. Higuchi, and C. R. Behl. Permeation of hairless mouse skin. I. Experimental methods and comparison with human epidermal permeation by alkanols. *J. Pharm. Sci.* 69:781–786 (1980).
6. P. Liu. *The Influences of Ethanol on Simultaneous Diffusion and Metabolism of β-Estradiol in Skin,* Ph.D. thesis, University of Utah, Salt Lake City, 1989.
7. B. P. Davis, E. Rampini, and S. L. Hsia. 17β-Hydroxysteroid dehydrogenase of rat skin, substrate specificity and inhibitors. *J. Biol. Chem.* 247:1407–1413 (1972).
8. R. C. Pirola. *Drug Metabolism and Alcohol,* ADIS Press, Sydney, University Park Press, Baltimore, 1977.
9. E. M. Sellers and M. R. Holloway. Drug kinetics and alcohol ingestion. *Clin. Pharmacokinet.* 3:440–452 (1978).
10. E. Rubin, H. Gang, P. S. Misra, and C. S. Liever. Inhibition of drug metabolism by acute ethanol intoxication. A hepatic microsomal mechanism. *Am. J. Med.* 49:801–806 (1970).
11. A. Sato, T. Nakajima, and Y. Koyama. Dose-related effects of a single dose of ethanol on the metabolism in rat liver of some aromatic and chlorinated hydrocarbons. *Toxicol. Appl. Pharmacol.* 60:8–15 (1981).